VOL. 11, NO. 6, MARCH 2016 ISSN 1819-6608
ARPN Journal of Engineering and Applied Sciences


www.arpnjournals.com

EFFECT OF THICKNESS ON RESIDUAL STRESS IN JOINING SIALON TO AISI 420

Nor-Nurulhuda MD. Ibrahim, Mokhtar Awang and Patthi Hussain
Mechanical Engineering Department, Universiti Teknologi Petronas, Bandar Seri Iskandar, Tronoh, Perak, Malaysia
E-Mail: nornurulhuda.mdi@gmail.com

ABSTRACT

Upon cooling down from a high fabrication temperature, residual stress will be generated within the joint of ceramic-metal components. The stress is originated from the difference in thermal expansion between ceramic and metallic substrates. The excessive internal stress always leads to premature failure of the joint due to cracking or debonding. In this work, distribution and magnitude of residual stress in cylindrical sialon-AISI 420 stainless steel-sialon joining have been evaluated numerically using ANSYS software by varying the thickness of the steel. The simulation has been performed under pure elastic deformation and several other assumptions. Three stresses are evaluated namely radial, axial, and shear stress. Most parts of the sialon are in compressive mode whereas majority of the regions in the steel have experienced tensile radial stress. The maximum tensile axial stress is located at the free edge of the sialon and at the centre of the joint. Meanwhile, the maximum shear stress is concentrated at the edge of the interface. Increasing the thickness of the steel has reduced the radial stress but the stress that acts in axial direction is increased. The radial and axial stress exhibit constancy in joining to steel with thickness more than 10.0 mm. Regardless of any thickness of the steel, the shear stress practically remains unchanged. Comparison to diffusion bonded sample has validated that the developed stress is lower than the fracture stress of the sialon since neither sialon nor reaction layer contains any crack.

Keywords: AISI 420 stainless steel, residual stress, sialon, and thickness.

INTRODUCTION

With rapidly increasing industrial demands nowadays, ceramic to metal joining becomes a popular trend in manufacturing activity. However, it is a challenge to obtain a high integrity joint between these materials due to their dissimilar cooling rate that cause inhomogeneous deformation at different region of the joint. Ceramics experience higher rate of lateral expansion since they possess low coefficient of thermal expansions (CTEs) where the values are about five times lower than steels. Dissimilarity in the rate of expansion leads to development of residual stresses which tend to be localized in the joint and reduce its load-carrying capacity, consequently increasing the tendency to fracture. Residual stresses are defined as self-equilibrating stresses within a stationary solid body without the presence of external forces on it [1]. Accumulation of excessive residual stress affects the joint severely since crack will be initiated at this region and propagates towards the ceramic. Ceramics can endure compressive stress but they will break under tensile stress since these materials possess low yield strength that contributes to their brittleness. In the case of steels, the tensile stress can be accommodated by the elastic and plastic deformation.

Numerous works on investigation of residual stress in the area of ceramic-metal joining that employ finite element method (FEM) have been carried out. Most of the works investigated the generation of residual stress in joining metal to Si3N4 or Al2O3 where the parameters that affect the generation of stress have been determined and discussed. Utilizing FEM has resulted in satisfactory description of the residual stresses distributions in the joints relative to the mechanical stress measurement methods [2–4]. A series of pioneering works in determining and describing the residual stress in ceramic-metal joining by finite element analytical model had been performed nearly three decades ago [5–6]. These earliest works studied the effect of geometrical parameters on the development of residual stress. The former work revealed that as the thickness of ceramic such as Si3N4 was increased, the maximum tensile stress in this material was also increased. Up to certain thickness and beyond, the stress started to show constant values. In the work of simulating the residual stress in Al2O3-Ni-HAYNES® 214TM joining, it was found that an increase in the thickness of the Al2O3 produced larger residual stress [4]. The maximum one was concentrated in the joint particularly at Al2O3-Ni alloy interface. Therefore, it was concluded that the critical part of the joint must be at the interface of the joined materials. In sialon-AISI 316 austenitic stainless steel joining, the work had shown that the magnitude of axial stress increased when joining sialon to thicker steel [7]. The gravity of the developed residual stress at the joint produced poor joint strength that would lead to early fracture of the component.

Attempt on the diffusion bonding of sialon to AISI 420 stainless steel produced no crack in the joint [8]. Due to difficulty in attaining the residual stress via the mechanical stress measurements, this work is conducted to numerically evaluate the distribution and magnitude of residual stresses in sialon-AISI 420 stainless steel joining with different thickness of steel by finite element analysis.

FINITE ELEMENT MODEL

Residual stresses in joining two different classes of materials were determined. The properties of the sialon and AISI 420 stainless steel that were utilized in the simulation are listed in Table-1.

Table-1. Properties of sialon and AISI 420 stainless steel.

Property	Sialon	AISI 420
Modulus of elasticity (GPa)	290	220
Poisson's ratio	0.23	0.27
CTE (10^{-6} K^{-1})	3.0	10.5
Thermal conductivity ($Wm^{-1}K^{-1}$)	21.0	24.9

The distribution and magnitude of the generated residual stress in the sialon-AISI 420 stainless steel joint was simulated using a commercial finite element software ANSYS version 15.0. The simulation was performed under several assumptions as the following:

- A two-dimensional model was sufficient to represent the three-dimensional structure geometry under investigation since both of the geometry and load can be completely described in one plane.
- Generation of residual stress was only caused by the difference in property of sialon and AISI 420 stainless steel where it did not involve any external mechanical load.
- Joining at 1473 K was assumed to form a perfect bond between the joined materials that resulted in perfect interface.
- Shrinking was allowed in the x- and y-direction to enable free deformation of the bonded materials.

A cylindrical shaped sialon-AISI 420 stainless steel-sialon arrangement was considered. As a result of the symmetry of the shape, only a quarter of the sample body was modelled. Modelling was performed by a two-step sequential coupled thermal-structural analysis. In the thermal-structure, the temperature distribution in the joined materials was acquired. Then, the nodal values were fed to the structural analysis as the only applied load. PLANE55 and PLANE182 with axisymmetric element behaviour were selected as the element for the respected thermal and structural analysis. As the maximum stress was expected to be formed near the joint interface and the free surface, mapped mesh with refinement had been imparted within these regions as illustrated in Figure-1. Pure elastic mode of the bonded materials was assumed to simplify the modelling.

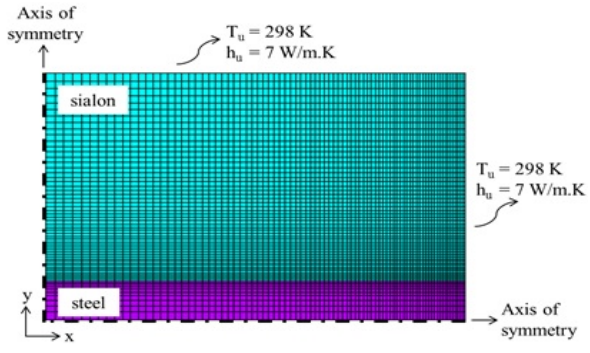

Figure-1. Schematic representation of the geometry, mesh configuration, and boundary conditions applied in the analysis.

Considering the boundary condition, the heat was only allowed to dissipate from the right side and top surface of the joined materials as illustrated in Figure-1. The only applied load on the model was thermal loading where it was in the form of temperature that comprised of cooling from 1473 K to 298 K. For convection heat transfer, film coefficient (hu) and bulk temperature of the still air (Tu) were set to 7 W/m.K and 298 K, respectively. The left side and the bottom part of the model were constrained in x- and y-direction, respectively whereas other surfaces remained free to allow bending upon cooling. The thickness of the steel was varied from 1 to 15 mm with different increment. Meanwhile, the sialon's thickness and diameters of the materials were fixed to 4 mm and 20 mm, respectively.

RESULTS AND DISCUSSION

During cooling down to ambient temperature, the imposed thermal loading has caused residual stress build-up as expansion and contraction took place in the joined materials. The distribution of the radial stress for joining sialon to steel with thickness of 1.5 mm is depicted in Figure-2. The negative sign that is shown on the values below the model indicates the compressive stress whereas the positive ones represent the stresses in tensile mode. Sialon experiences the compression where the maximum compressive stress is concentrated near the edge of the joint with a value of 610 MPa. Meanwhile, the steel is under tensile mode where the stress has increased towards the centre of the joint with the maximum value of 946 MPa. Compressive stress with a value of 91.3 and 264 MPa are developed at the free surface of the sialon and the steel, respectively. Most parts of the sialon are dominated by the compressive stress of 264 MPa. The pattern is in agreement with the model that has been proposed by another researcher [9].

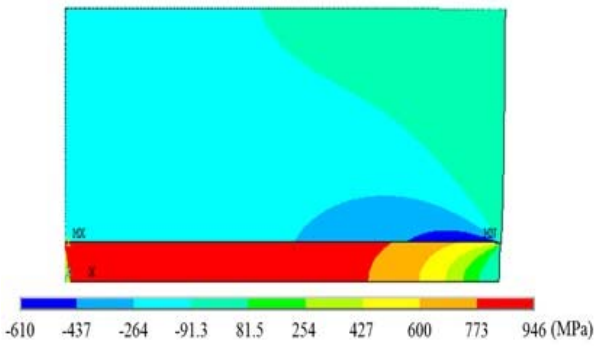

Figure-2. Radial stress distribution across the sialon-steel joint.

Evaluation of stress in y-direction has produced the distribution of the axial stress as presented in Figure-3. It shows the distribution of stress in joining sialon to 1.5 mm-thick-steel. The maximum tensile axial stress with a value of 187 MPa is located at the interface of the base materials. In addition, it is distributed at the edge of free

surface in sialon. From Figure-3 also, approximately more than 80% of the steel experiences the axial stress in tensile mode. It spread towards the centre of sialon that is located close to the interface. The free surface of the steel has experienced very high compressive stress which is 1030 MPa, near the edge of the joint. However, it only covers a very small region of the steel. Meanwhile, compressive stress with a value of 83.8 MPa is generated in most regions of the sialon ceramic.

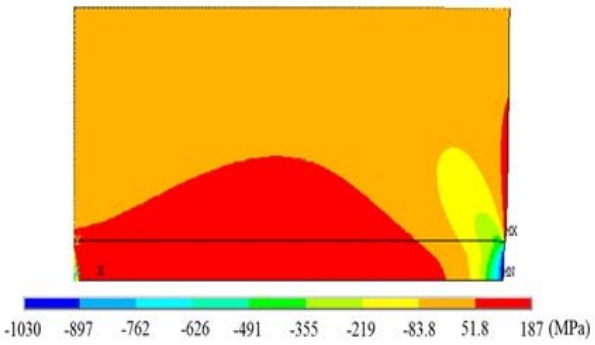

Figure-3. Axial stress distribution across the sialon-steel joint.

The distribution of shear stress in the joined materials with a steel having thickness of 1.5 mm is shown in Figure-4. At the edge of the joint, maximum tensile stress is formed with a value of 374 MPa. This maximum stress is only distributed in a small region of the bonded materials. The contour plot of the distribution becomes gradually larger as moving away from the edge but the magnitude of the stress is reduced. The minimum compressive stress is 13.1 MPa. It is distributed at the free surfaces of the materials and towards the centre of the joint. It occupies about 50% of the parts in sialon and the steel. The maximum tensile shear stress is concentrated at the edge of the joined interface since this region is always prone to detachment as compared to the centre of the joint.

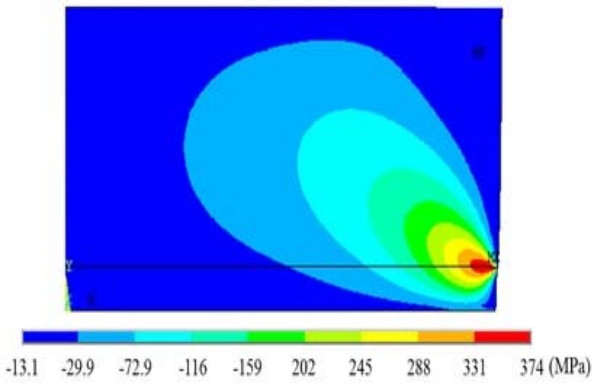

Figure-4. Shear stress distribution across the sialon-steel joint.

The distribution and magnitude of residual stress in a sialon-steel joint that undergoes cooling from a high temperature is not uniform as illustrated in Figure-2 to Figure-4. Regardless of any steel thickness, the patterns of the residual stress distributions are quite similar. They only have small difference in the contour plot of the coverage area. Therefore, Figure-2 to Figure-4 can be used as the reference for the stress distribution in any thickness of steel. In general, sialon and steel are subjected to radial stress in compressive and tensile mode, respectively. The maximum tensile axial stress is located at the free edge of sialon and at the interface where the magnitude has affected the strength of the joint. Meanwhile, the highest shear stress in tensile mode is concentrated at the end of the interface, close to the edge of the free surfaces. In comparison to the diffusion bonded sample, the edges of the joined materials easily become de-bonded or detached due to the unjoined edge or the presence of other defects for example interface flaw [10]. For this reason, high possibility of cracking may be initiated at the interface that followed by propagation towards the sialon.

The distributions of stresses which have been attained are in accordance with the past works. The distributions in Al2O3-Ni-HAYNES® 214TM biomaterials joint [11] had shown patterns that possessed some similarities with the obtained stresses in this work. In the x-direction, compressive and tensile stresses were developed in the ceramic and metal, respectively where the largest one was generated at the interface of the joint. On the other hand, the free edge of the alumina ceramic perpendicular to the joint had the highest tensile axial stress. Meanwhile, the shear stress was concentrated at the edge of the joined materials' interface. Also, similar pattern had been observed in the work of determining the residual stress in Si3N4-steel joint [5]. The maximum stresses were formed at the free edge of Si3N4 and at the interface of the bonded materials as well. Stress in y-direction that located at the free surface of the sialon was in tensile whereas the free end of the steel experienced compressive mode. These modes of stresses are developed at those regions since cooling has caused the contraction of the steel as illustrated in Figure-3. The generated compressive stress at the free surface of the steel has been triggered by the effect of yielding in the steel. Bending that occurs in the sialon is to balance the bending moment when the steel shrinks during cooling [12]. The distribution of residual stress in sialon-AISI 430 ferritic stainless steel joining [9] is also in agreement with the current work. Sialon experienced axial stress in tensile mode at the free surface whereas the free end of the steel was in compression. The work had shown that high tensile stress was developed at the centre of the joint.

Simulation of the residual stress by increasing the thickness of the steel has resulted in reduction of the maximum tensile radial stress but it does increase in the axial stress whereas shear stress remains constant as demonstrated in Figure-5. The highest radial stress is attained in joining sialon to 1.0 mm-thick-steel with a value of 988 MPa. The stress is gradually decreased where the lowest one with a value of 621 MPa has been attained in joining to the steel having thickness of 8.0 mm. Around

10.0 mm-thick of the steel, the stress starts to show constancy with a value of 601 MPa. Further increasing the thickness by joining to thicker steel produce only a slight difference of the radial stress since the value is 603 MPa. The percentage of increase is 0.33% at which it can be disregarded. The opposite trend is observed in axial stress where the value has increased as the steel thickness is increased. Joining to thicker steel has resulted in the increase of the tensile stress at the free end of the sialon and at the centre of the joint. Employing 1.0 and 10.0 mm-thick-steel generate stress with a value of 136 and 531 MPa, respectively. The axial stress exhibits constancy when sialon is bonded to 12.0 mm-thick-steel and beyond. Meanwhile, joining to any thickness of the steel does not influence the shear stress. The stress shows almost constant values since they are in the range of 369 to 377 MPa where the difference is less than 2.20%.

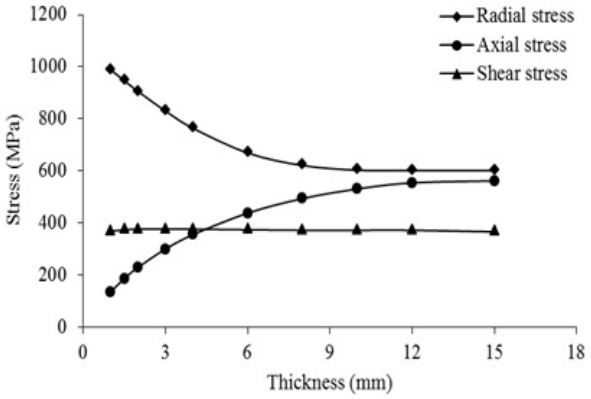

Figure-5. The maximum tensile stresses by varying the thickness of the steel.

From the findings that are presented above, thickness of the steel plays important role in generation of residual stress within a sialon-steel joint. From Figure-5, the residual stress in the x- and y-direction is the only two affected stresses when joining to steel with thickness less than 10.0 mm. The thickness of the steel influences the bending curvature of the joined materials. In thicker steel, it will experience larger bending curvature where it has resulted in higher tensile axial stress at the free edge of the sialon. According to Figure-5, constant stress is generated beyond certain thickness of the steel and this implies that the bending curvature has reached its limit due to stress relaxation [13]. Joining sialon to thinner steel produces smaller bending curvature that resulted in lower axial stress. Among the three evaluated stress, the axial stress which acts along the y-direction is the most important one as the increase in the tensile stress will directly affect the sialon. As illustrated by Figure-3, the free edge of sialon and at the centre of the joint experience the maximum tensile axial stress. Sialon does not have the ability to withstand large tensile stress since it is a brittle material due to its lower yield strength as compared to the steel.

Without considering the reaction layer, the simulation has resulted in low axial stress at the interface. In 1.5 mm-thick-steel, it produces stress with a value of 187 MPa which is very much lower than the fracture stress of the sialon (i.e. 825 MPa). Thus, the joint will not fail when sialon is bonded to AISI 420 stainless steel and this has been further supported by the finding attained from the diffusion bonded sample where no crack formation at the interface layer and the sialon as shown by the optical micrograph in Figure-6.

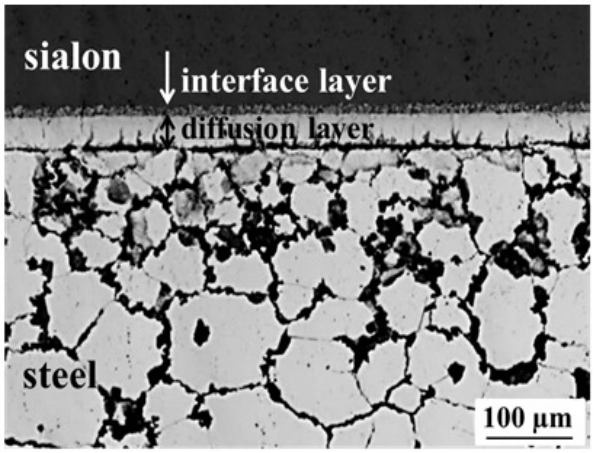

Figure-6. Optical micrograph of joining sialon to 1.5 mm-thick AISI 420 stainless steel.

Although the reaction layer is not taken into consideration since it has been assumed that the bonded materials will form a perfect interface, the residual stresses which have been attained are still in agreement with the diffusion bonding experiment [8]. In the work, the joint does not show any form of crack. It has been predicted that joining sialon to AISI 420 stainless steel will be possible since the materials possess CTE that does not differ too much as given in Table-1. A huge difference of this property will cause large development of the internal stress as it happened in the case of joining sialon to austenitic stainless steel [14]. Meanwhile, joining sialon to ferritic stainless steel was a successful attempt. These materials were able to be bonded because their possessed smaller difference of CTE as compared to austenitic stainless steel. The CTE of the ferritic and austenitic stainless steel were (16.87 x 10-6) and (22.56 x 10-6) K-1, respectively. High residual stress caused cracking in the assembly but this defect was not observed in joining sialon to ferritic stainless steel.

The accuracy of residual stresses obtained through FEM in this work will not be quantitatively 100% in agreement with the results attained via mathematical calculation or the mechanical stress measurements such as diffractions or indentation fracture methods since the plastic behaviour of the steel is not taken into account. However, the analysis still can be applied as a simple guideline that is able to provide a valuable framework in assessing the developed stress within the sialon-AISI 420 stainless steel joint as mechanical stress measurement in determining the residual stress has yet to be carried out in

this particular joining. In fact, several works on evaluating the state of residual stress in the ceramic-metal joining have carried out the simulation based on this simple elastic method [7],[15],[16]. The calculated stresses from numerical works are always different from the measured ones. Several possible reasons have been identified for causing this discrepancy. They are residual stress relaxation, recovery process during cooling, and assumptions that are taken into consideration for example adoption of two-dimensional rather than three-dimensional model [17]. Limiting the assumptions by conducting the simulation close to the real problem and incorporating the three-dimensional analysis have greatly improved the results [2]. From the previous research also, the difference has been caused by the effect of interfacial reaction on the joint's properties [7]. By considering the reaction layer in the analysis, it will produce more realistic values of the generated stresses since the joint acts as a buffer zone to accommodate the internal stresses.

CONCLUSIONS

Axial, radial, and shear stress are the three evaluated stresses. At the free end of the sialon and the centre of the joint, these regions experience stress in tensile mode. In general, increasing the thickness of the steel produces lower radial stress but the opposite occurs on the axial stress that indicates the latter stress has higher influence in determining the strength of the joint. Constant values of stresses are attained in thicker steel due to the effect of bending-induced stress relaxation which has been provided by the steel. The magnitudes of all stresses are gradually reduced as moving further away from the interface. Due to the extreme difference of stress, the critical region is located at the interface of the bonded materials. Regardless of any thickness of the steel, the shear stress practically remains unchanged. The attained residual stresses will not cause fracture in the joint as verified by no cracking in the joint of the diffusion bonded sialon to AISI 420 stainless steel.

ACKNOWLEDGEMENTS

The authors would like to extend the gratitude to Universiti Teknologi PETRONAS by providing the facility to perform the simulation work. Also, many thanks to Ministry of Higher Education for financing the research under grant of ERGS 015 3AB-I21.

REFERENCES

[1] M. T. Hutchings, P. J. Withers, T. M. Holden, and T. L. Lorentzen. 2005. Introduction to the characterization of residual stress by neutron diffraction. Taylor and Francis Group. pp. 1.

[2] M. Kurita and K. Yoneda. 1993. Three-dimensional FEM residual stress analysis for ceramic-metal joint plate. Transactions on Engineering Sciences. 2: 29-38.

[3] S. B. Lee and J. H. Kim. 1997. Finite element analysis and x-ray measurement of residual stresses of ceramic metal joints. Journal of Materials Processing Technology. 67: 167-172.

[4] M. L. Hattali, S. Terekhina, F. Ropital, N. Mesrati, and D. Tréheux. 2009. Optimization of fabrication parameters of alumina/nickel alloy joints for high-temperature application. Materials Science and Engineering. 5: 1-7.

[5] K. Suganuma, T. Okamoto, M. Koizumi, and M. Shimada. 1985. Effect of thickness on direct bonding of silicon nitride to steel. Journal of the American Ceramic Society. 68: 334-335.

[6] K. Suganuma, T. Okamoto, M. Koizumi, and K. Kamachi. 1987. Influence of shape and size on residual stress in ceramic-metal joining. Journal of Materials Science. 22: 3561-3565.

A. Abed, P. Hussain, I. S. Jalham, and A. Hendry. 2001. Joining of sialon ceramics by a stainless steel interlayer. Journal of the European Ceramic Society. 21(16): 2803-2809.

[7] N. N. Md. Ibrahim, P. Hussain, and M. Awang. 2014. Effect of nitriding on reaction layer of diffusion bonded sialon to AISI 420 martensitic stainless steel. Applied Mechanics and Materials. 660: 178-184.

[8] C. S. Hassan. 2011. Stress analysis using finite element method on sialon/AISI 430 ferritic stainless steel joint. Universiti Teknologi PETRONAS, Tronoh, My.

[9] J. Lemus-Ruiz, C. A. León-Patiño, and R. A. L. Drew. 2006. Self-joining of Si3N4 using metal interlayers. Metallurgical and Materials Transactions A. 37: 69-75

[10] L. Hattali, V. Stephane, F. Ropital, N. Mesrati, and D. Tréheux. 2009. Effect of thermal residual stresses on the strength for both alumina/Ni/alumina and alumina/Ni/nickel alloy bimaterials. Journal of Materials Science. 44: 3198-3210.

[11] C. H. Hsueh and G. A. Evans.1985. Residual stress in metal/ceramic bonded strip. Journal of the American Ceramic Society. 68(5): 241-248.

[12] J. Mencik. 1995. Mechanics of components with treated or coated surfaces. Dordrecht: Kluwer Academic Publishers.

[13] P. Hussain. 1997. Diffusion bonding of sialon and stainless steel. University of Strathclyde, Glasgow, UK.

[14] J. X. Zhang, R. S. Chandel, Y. Z. Chen, and H. P. Seow. 2002. Effect of residual stress on the strength of an alumina-steel joint by partial transient liquid

phase (PTLP) brazing. Journal of Materials Processing Technology. 122: 220-225.

[15] X. Shen, Y. Li, U. A. Putchkov, J. Wang, and W. Huang. 2009. Finite-element analysis of residual stresses in Al2O3-TiC/W18Cr4V diffusion bonded joints. Computational Materials Science. 45: 407-410.

[16] H. Li, L. Z. Sun, J. B. Li, and Z. G. Wang. 1996. X-ray stress measurement and FEM analysis of residual stress distribution near interface in bonded ceramic/metal compounds. Scripta Materialia. 34(9): 1503-1508.